E3S Web of Conferences **730**, 05014 (2026) https://doi.org/10.1051/e3sconf/202673005014
Soft Soils 2026

Constructing a large diameter open caisson in soft clay

Laura Willis [1,2*], *Peter* Hensman [3], *Declan* Phillips [1], and *Ronan* Royston [1,2]

[1] Faculty of Science and Engineering, School of Engineering, University of Limerick, Co. Limerick, Ireland
[2] Ward and Burke Construction Ltd., Stradbally East, Kilcolgan, Co. Galway, Ireland
[3] Ward and Burke Construction Ltd., 26 Ivor Pl, London, United Kingdom

Abstract. This paper presents the design, construction and monitoring of a 28 m internal diameter caisson located in the flood plain of the River Shannon in Athlone, Ireland. Under a self-weight exceeding 5000 tonnes the caisson ultimately penetrated through over 10 m of soft alluvial clays and silts with undrained shear strengths between 7.5 and 28 kPa. The caisson then passed through strata of coarse-grained soils before partially bearing on limestone bedrock. The challenging ground conditions necessitated a robust design approach to address the risk of premature bearing capacity failure and excessive movements of the structure during construction. To address these concerns, the caisson interior was surcharged with 3000 tonnes of clean stone, and two complementary analytical methods were employed to predict soil-structure performance. The first employed an empirical bearing capacity analysis accounting for a tapered caisson toe in clay, and the second was a 2-D finite element analysis. Both approaches predicted the structure would penetrate the clay before the 15.4 m high, 1.6 m thick wall construction was complete. The Eurocode 7 observational method was adopted to monitor construction and was informed by real-time instrumentation data. The structure did not penetrate the clay during caisson construction as predicted; this may be attributed to the selection of conservative design parameters, natural variability in the soil profile and soil strengthening due to consolidation induced by the clean stone surcharge. This case study highlights the challenges of predicting soil-structure interaction in soft ground and provides practical insights on the design, construction and monitoring of large-diameter caissons in complex geological settings.

1 Introduction

Rapid urbanisation in Ireland, combined with a persistent housing crisis and the need for compliance with EU wastewater directives, has intensified the demand for underground civil infrastructure [1]. To expand wastewater capacity within constrained urban environments, large-diameter caissons are increasingly employed as key structural elements for deep pumping stations and stormwater attenuation systems.

Caissons can be constructed by using segmental pre-cast elements and hydraulic jacks as kentledge. An alternative method is by sinking in-situ concrete walls through the ground. This is achieved by internally excavating the ground in the structure causing the soil to fail in bearing while the structure itself provides the kentledge. Sinking of caissons requires controlled movements into the ground to ensure verticality while also minimising friction at the soil-structure interface [2].

Predicting the trigger load for caisson penetration in very soft alluvial clays remains highly uncertain due to conservative empirical approaches, soil variability, and limited full-scale data. This paper examines the determination of the bearing load required to initiate caisson penetration in very soft alluvial clays and silts for maintaining stability during temporary construction conditions. Trigger loads were defined using two independent analytical approaches, with controlled bearing failure intended only after completing the above ground construction of the caisson. Installation proceeded under an observational framework in accordance with Eurocode 7, supported by real-time monitoring to manage displacement risk and associated contingency plans. A full-scale case history is presented to assess the reliability of trigger load prediction and the role of observational control in caisson installation in extremely low-strength ground.

1.1 Features of an in-situ open caisson

Typical features of an in-situ open caisson include an angled bearing face and a steel cutting shoe to facilitate penetration into the ground, these are illustrated in Fig. 1. The cutting shoe is of greater diameter than the external wall of the structure to create an annulus along the external circumference of the structure. This annulus is pumped with a lubricating fluid, commonly bentonite slurry, to minimise soil-structure friction generation along the external wall [3]. Lubrication lines are cast into the caisson wall to enable the pumping of bentonite slurry. The self-weight of the caisson walls provides the downwards kentledge while the soil at the bearing face and friction along the external wall provide the resistance. If the downwards forces are nominally greater than the

*Corresponding author: Laura.Willis@wardandburke.com

resistance forces, then the shaft sinks into the ground in a controlled manner. Conventional design methods often assume conservative soil parameters, which can lead to overestimation of required driving loads and, consequently, to overly robust wall sections [2,3].

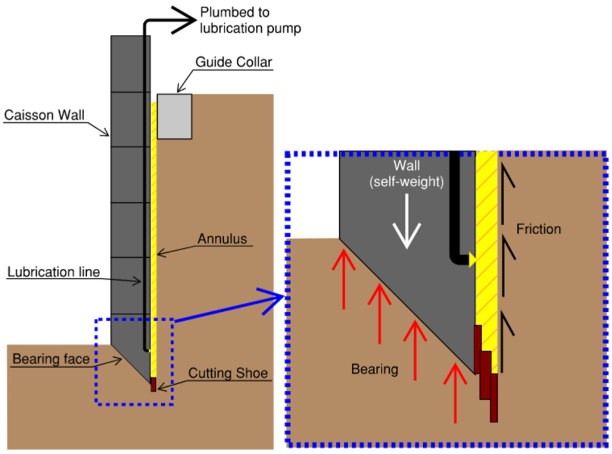

Fig. 1. Section through caisson wall with notable elements labelled and zoomed-in details at base of structure.

1 Athlone main drainage scheme

1.1 Project overview

The Athlone Main Drainage Scheme (AMDS) is a major Uisce Éireann initiative intended to upgrade the wastewater network serving Athlone, County Westmeath. The project aims to reduce the risk of urban sewer flooding and eliminate noncompliant combined sewer overflows to the River Shannon, which is designated an environmentally sensitive area [4,5]. This project also increases the capacity of the network to accommodate projected population growth.

This study focuses on the construction of the new Golden Island Pump Station (GIPS), a key component of the AMDS. The facility is being constructed as a 31.2 m external diameter open caisson with 1.6 m thick in situ reinforced concrete walls, providing an operational storage capacity of approximately 4,500 m³. The shaft is located at Golden Island, positioned on the east bank of the River Shannon, south of Athlone town centre. Fig. 2 (a) illustrates its geographical context and Fig. 2 (b) is an aerial image of the caisson during construction.

(a) (b)

Fig. 2. (a) Shaft location indicated on a map of Athlone, and (b) Aerial photograph of GIPS during construction [6].

1.2 Ground conditions

The ground conditions at the GIPS site were established from site investigations comprising 15 boreholes (BHs) and 11 cone penetration tests (CPTs), supported by associated field and laboratory measurements. The BHs within a 50 m radius of the centre of the shaft were utilised to establish a representative ground model as illustrated in Fig. 3. The inferred ground model's stratigraphy and site investigation results are presented in Fig. 4.

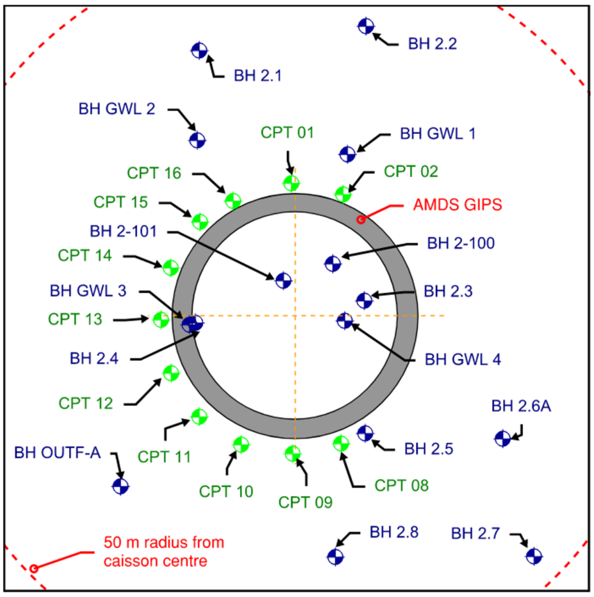

Fig. 3. BHs and CPTs located within a 50 m radius from the centre of the caisson.

The subsurface profile consists of approximately 5.3 m of made ground (MG), comprising topsoil and historic landfill materials, overlying an average of 10.3 m of normally consolidated alluvial clays and silts (ACS). Beneath the ACS lies approximately 3.6 m of granular glacial till (GT-G), underlain by limestone bedrock (LST). The caisson structure before and after sinking is sketched adjacent to the ground model stratigraphy in Fig. 4 (a). Variability in the stratigraphic boundaries are illustrated on this model by error bars representing the observed range of layer elevations surrounding the caisson.

The ACS layer comprises predominantly very soft clays with their natural moisture content (NMC) tending towards the liquid limit (LL) as shown in Fig. 4 (f). Measured pore water pressure (PWP) exceeds hydrostatic conditions throughout the ACS layer (Fig. 4 (d)), indicating an undrained low-permeability fine-grained soil. A transition towards hydrostatic pressures is observed upon entering the GT-G layer.

The undrained shear strength (s_u) of the ACS layer was estimated from the CPT results using the bearing capacity method described in Eq. 1 [7,8].

$$s_u = \frac{q_t - \sigma_{v,0}}{\mathrm{N_{kt}}} \tag{1}$$

Where q_t is the corrected cone resistance, $\sigma_{v,0}$ is the total overburden stress and $\mathrm{N_{kt}}$ is an empirical cone factor. Strength profiles are plotted in Fig. 4 (e) for $\mathrm{N_{kt}}$ values of

15 and 20, as recommended for cohesive fine-grained soils [8], with an N_{kt} value of 20 adopted in previous studies for very soft clays within the Athlone area [7]. Corrected field shear vane results and two suggested design strength lines are plotted in Fig. 4 (e) and described in Table 1. Design line (DL) 1 is the more conservative line utilised by the design team for GIPS, while DL 2 reflects a strength trend corroborated by field shear vane tests between elevations 28 and 33 mOD, with a linear increase at greater depths inferred from CPT data.

Table 1. Design lines for s_u inferred from SI.

Design line	Elevation (mOD)		Su (kPa)
	Upper Elev.	Lower Elev.	
1	37.99	30.99	7.5
	30.99	19.99	Linear increase to 28
2	37.99	29	16
	29	19.99	Linear increase to 40

1.3 Construction sequence

The construction sequence for the GIPS caisson is described in 10 phases summarised in Table 2. Two circular cofferdams constructed from sheet piles were installed concentrically around the shaft location, with radii extending 2 m and 3 m beyond the external caisson wall. The top of the cofferdams were braced by a reinforced concrete ring beam installed between the two sheet pile rings. The interior of the cofferdam was excavated to approximately 30 mOD, before caisson construction commenced.

After this excavation, the internal level was filled with a 1 m layer of clean stone (6”) to provide a working platform on the soft clay, before pouring a level bearing pad on the stone. A steel cutting shoe was positioned on this pad to establish the overcut required for external wall lubrication during sinking. Inside the cutting shoe, precast concrete wedges were installed to form the 45° tapered internal bearing face for the first concrete lift.

All wall pours of the structure, totalling 15.37 m in height and applying approximately 360 kPa/m pressure to the ground, were completed before sinking commenced as illustrated in Fig. 5. To support the caisson self-weight, a further 2.5 m thick layer of clean stone (6”) was placed inside the shaft after the first wall pour, contributing approximately 3000 tonnes of additional surcharge to the underlying clean-stone working platform. This surcharge load was in place for approximately 2.5 months during the construction period.

A single 5.4 m deep guide collar, supported by piles, was constructed to aid caisson alignment during sinking. Once the structure reached its final height, an excavator was positioned inside the shaft to excavate the soil around the interior perimeter to initiate the sinking phase.

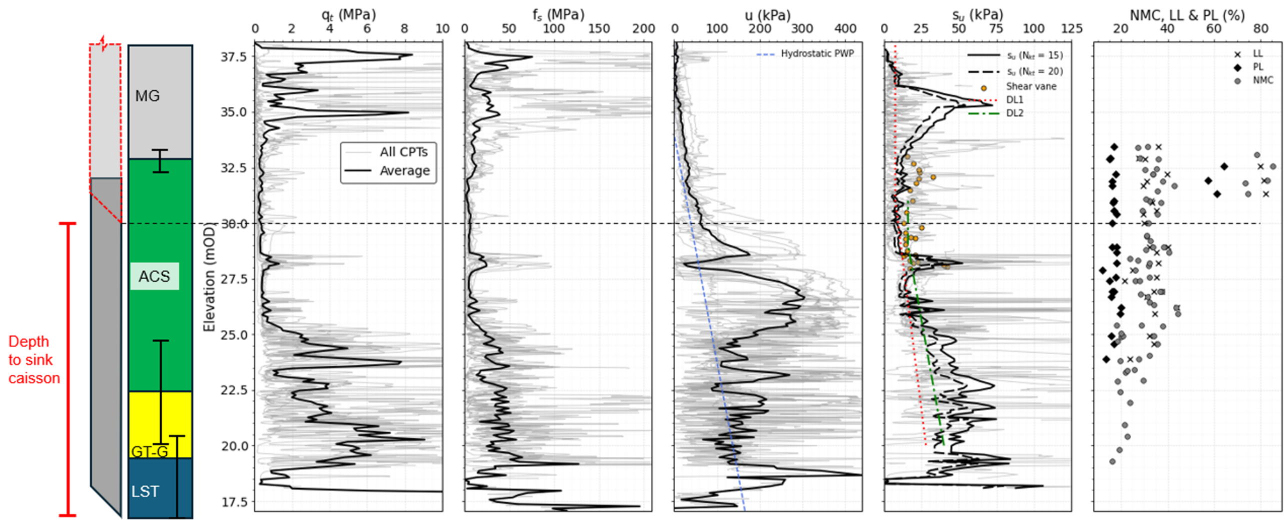

(a) (b) (c) (d) (e) (f)

Fig. 4. Site investigation summary: (a) Caisson position before and after sinking relative to the interpreted site stratigraphy; (b) corrected CPT cone resistance, q_t profile; (c) CPT sleeve friction, f_s profile; (d) PWP profile, including the hydrostatic line; (e) undrained shear strength, s_u, profiles derived from CPT correlations, field vane test results, DL1 and DL2; and (f) NMC and Atterberg limit profiles.

Table 2. Caisson construction sequence phases.

Step No.	Construction Activity	Start date	End date	Duration (workdays)
1	Install sheet piles	3rd May 2023	7th June 2023	26
2	Pour ring beam	17th July 2023	17th July 2023	1
3	Excavate internally to 30 mOD	8th Aug. 2023	1st Sept. 2023	19
4	Fill clean stone for working platform and form bearing pad	30th Aug. 2023	18th Sept. 2023	13
5	Install cutting shoe	18th Sept. 2023	18th Sept. 2023	1
6	Position pre-cast wedges	20th Sept. 2023	22nd Sept. 2023	3
7	Wall pour 1	23rd Sept. 2023	10th Oct. 2023	13
8	Surcharge internally with clean stone	16th Oct. 2023	19th Oct. 2023	4
9	Guide collar pour	16th Oct. 2023	16th Oct. 2023	1
10	Wall pours 2 -7	19th Oct. 2023	20th Dec. 2023	49

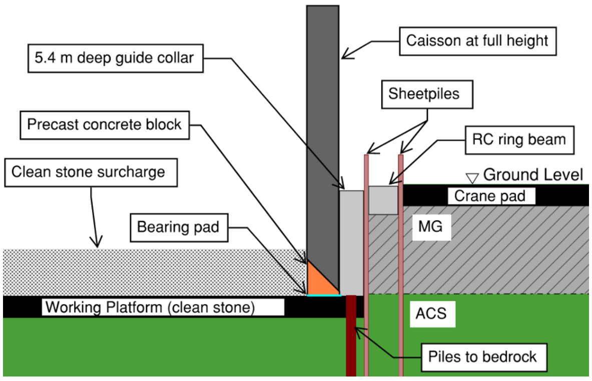

Fig. 5. Annotated sketch of section through GIPS post construction and pre-sinking.

2 Bearing capacity assessment under temporary conditions

This section outlines the analytical methodologies employed to determine the critical trigger loading for initial caisson penetration. The ultimate bearing capacity described in the next section was estimated using closed-form analytical solutions, and a 2-D finite element analysis (FEA) conducted within PLAXIS 2D.

2.1 Bearing capacity assessment

To facilitate wall construction, a 3.5 m thick layer of clean stone surcharge was placed inside the caisson for a period of approximately 10 weeks. The clean stone properties used in the analysis are summarised in Table 3.

Table 3. Clean stone properties [9].

Parameter	Value	Unit
Unit weight ($\gamma_{\text{clean stone}}$)	22	kNm^{-3}
Angle of friction (ϕ)	40	$^{\circ}$(degrees)

To predict the undrained bearing load, unfactored actions together with characteristic soil and material properties were employed. The loading from the structure (q_1), poured in 7 lifts (Table 4), assumed the unit weight of concrete as 25 kNm^{-3}.

Table 4. Cumulative loading of structure by incremental pouring of concrete walls.

Pour No.	Pour height (m)	Bearing Load, q_1 (kPa/m)
1	2.475	41.5
2	2.4	101.5
3	2.4	161.5
4	2.4	221.5
5	2.4	281.5
6	0.895	303.9
7	2.4	363.9
Total	15.37	363.9

The initial bearing capacity of the soil was based on a rectangular footing, due to the installation of the wedge shaped precast concrete blocks (see Fig. 5) positioned around the internal circumference of the caisson. The bearing pressure (q_2) acting on the soft clay was based on a load dispersion through the working platform according to Eq. 2 [10].

$$q_2 = q_1\left(\frac{B}{B+d}\right) \tag{2}$$

Where B is the footing width and d is the thickness of the clean stone working platform beneath the precast concrete blocks. The bearing capacity (R/A') of the soft clay was calculated using Eq. 3 from Annex D of Eurocode 7 [11].

$$\frac{R}{A'} = (\pi+2)s_u b_c s_c i_c + q \tag{3}$$

Where b_c, i_c and s_c are 1 and q is calculated based on the clean stone surcharge. Once the caisson punches through the stone fill, it is assumed the precast concrete blocks rotate away from the caisson bearing face as it penetrates the clay and the bearing load returns to q_1. The bearing response of the clay (q_{rd}) for a tapered base with angle β (°) is then evaluated using Eq. 4 [12], with the relevant parameters defined in Fig. 6 and the numerical values summarised in Table 5.

Table 5. Input parameters used in Eq.4.

Parameter	Value	SI Units
s_u	defined in Table 1	kPa
$N_{c,\beta,axi}$	evaluated using Eqs. 5–7	-
B	1.6	m
γ_s	18	kNm^{-3}
β	45	°
h	0	m
q_s	76.45	kPa

$$q_{rd} = s_u N_{c,\beta,\text{axi}} + \frac{B\gamma_s}{2\tan\beta} + h\gamma_s + q_s \tag{4}$$

Where q_s is the surcharge load, γ_s is the unit weight of the soil and $N_{c,\beta,axi}$ is a modified bearing capacity factor accounting for the influence of the tapered angle at the base, embedment depth within the clay, and axisymmetric caisson geometry, evaluated using Eqs. 5, 6 and 7. The embedment depth h was initially taken as zero and incrementally increased until equilibrium was achieved.

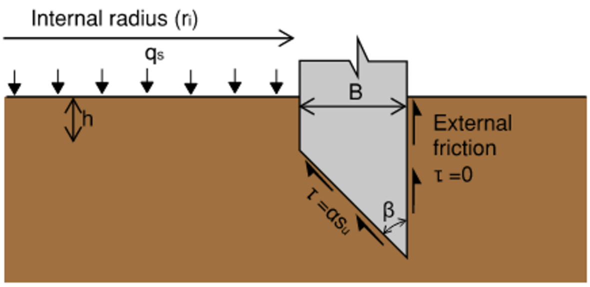

Fig. 6. Parameter definition for Eq. 4 [12].

$$N_{c,\beta,\text{h=0}} = \left[2\left(\frac{\beta}{180^{\circ}}\pi\right)+2\right] + \left[\alpha + \frac{\pi-4}{2}\alpha^2\right] + \left[\frac{\alpha}{\tan\beta}\right] \tag{5}$$

$$N_{c,\beta} = N_{c,\beta,\text{h=0}} + \left[\frac{\left(h/B\right)^{0.452}}{\cos\beta + 0.133\alpha}\right]$$

 https://doi.org/10.1051/e3sconf/202673005014

$$\leq N_{c,\beta,\mathrm{h=0}} + \left[\frac{\left(h/B\right)^{0.452}}{\cos(50°) + 0.133\alpha}\right] \quad (6)$$

$$N_{c,\beta,\mathrm{axi}} = \left[\frac{8}{9} - \frac{2}{3}\left(\frac{h}{B}\right)\right]\left(B/r_i\right) + N_{c,\beta} \leq A_\mathrm{b}\ln\left(B/r_i\right) + B_\mathrm{b}\left(B/r_i\right) + C_\mathrm{b}\left[\left(\frac{\beta}{180°}\pi\right) - \frac{\pi}{6}\right] + \frac{\alpha}{\tan\beta} + \alpha\left(B/r_i\right) \quad (7)$$

Where the parameters A_b, B_b, and C_b are constant values of -2.162, 4.277 and 2.52, respectively. The formulation is applied iteratively to determine the embedment corresponding to equilibrium between the applied load and the increasing bearing resistance as the caisson penetrates the clay. This procedure provides a prediction of the embedment depth for a given load case, enabling estimation of the depth at which the structure stabilises once the trigger load has been reached.

This approach assumes that the bentonite slurry injected into the annulus provides effective lubrication between the caisson wall and the adjacent soil, thus making the interface friction insignificant. This assumption is supported by field measurements from an instrumented caisson in comparable ground conditions in the UK [13].

Interactions between the surcharge clean stone and the caisson wall are not explicitly considered. Frictional resistance along this interface is expected to be negligible, and any potential contribution is further reduced by inward failure of the precast concrete blocks at the tapered edge, which disrupts the development of sustained interface resistance at this location. The results of this analysis are illustrated in Fig. 9 and discussed in Section 4.1.

2.2 Finite element analysis (FEA)

A two-dimensional finite element model was developed in PLAXIS 2D to simulate the caisson wall bearing under axisymmetric conditions. The model geometry comprised a radial section through the caisson wall and soil stratigraphy, with the vertical model boundary defined as the axis of symmetry, as shown in Fig. 7. The soil stratigraphy presented in Fig. 4 (a) was used in the FEA model. The ACS layer was modelled using the Mohr-Coulomb (MC) constitutive model with a PLAXIS undrained B type analysis, which accommodates a defined undrained shear strength profile [14]. This approach was adopted as a first-order representation, reflecting the limited availability of data required to define the parameters necessary for more advanced models. Two models were developed to simulate the caisson wall bearing using the two ACS layer strength profiles, DL 1 and DL 2, with depth (z) as defined in Table 1. The density, initial soil state and MC model input parameters for the ACS layer were inferred from the results of in situ and laboratory tests carried out during the site investigation works and are summarised in Table 6.

The finite element mesh was generated with local refinement in the vicinity of the bearing-soil interface and within zones experiencing higher stress and strain gradients, while a coarser discretisation was adopted at greater distances to optimise computational efficiency. Boundary conditions were assigned to restrict horizontal displacements along the vertical axisymmetric boundary and the sheet pile wall.

Table 6. Summary of density, initial soil state and MC model input parameters.

Soil unit weight, γ	18 kNm^{-3}
Saturated soil unit weight, γ_{sat}	20 kNm^{-3}
Secant stiffness, E_{50}	10 MPa
Poisson's ratio, ν	0.25
Undrained shear strength, s_u	7.5 + 2.5z kPa (DL 1) 16 + 4.4z kPa (DL 2)
Lateral earth pressure coefficient at rest, K_0	0.5

The caisson wall was represented by applying its self-weight as a line load and by constraining lateral displacement along the internal caisson wall using a zero-deflection boundary condition. Loading was applied incrementally to model the sequential caisson wall construction method (Table 4). The undrained scenario was modelled with no consolidation stages incorporated as a conservative assumption, providing a lower-bound estimate of bearing capacity for design safety.

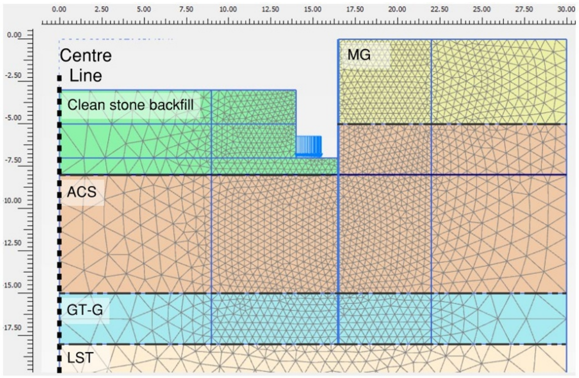

Fig. 7. PLAXIS 2D caisson bearing model setup with soil stratigraphy labelled.

2.3 On-site methodology

GIPS was classified as a Category 3 structure according to Eurocode 7 [11], therefore as a risk mitigation measure instrumentation was utilised to analyse the performance of the structure in real time [15]. The Ward and Burke liquid level system (LLS) was installed to monitor any caisson movements, reducing the risk of any uncontrolled structure displacement and providing early warning of imminent movement by detecting initial creep.

The system is configured such that an excavator operator can log into an online platform displaying real-time LLS data within the machine, accessing the user interface shown in Fig. 8. This interface guides the excavator driver during caisson sinking by providing the cutting shoe elevation plotted against time and indicating the verticality of the structure using a red-green ("stop-go") system for each quarter point of the shaft. This LLS consists of five pressure transducers, four cast into the structure at quarter points and a benchmark pressure transducer at a known stationary elevation all contained within an open loop system connected to a header tank filled with water. Willis et al. (2024), Royston (2020) and Sheil et al. (2018) provide detailed descriptions of the configuration and installation of the LLS [3,6,13,16].

The LLS data was used to manage construction risk by continuously monitoring vertical displacement in real time at a sampling frequency of 1 Hz. Displacements were closely monitored, particularly as applied loads approached the predicted trigger loads derived from the analyses presented in sections 3.1 and 3.2. Incremental concrete wall pours (Table 4) were placed in circular lifts over a minimum duration of six hours, producing an average concreting rate of approximately 400 mm h^{-1} (≈16 kPa m^{-1} h^{-1}). This relatively slow loading rate limited abrupt stress increases and allowed construction activities to be monitored, identifying any movements indicative of mobilisation of bearing failure.

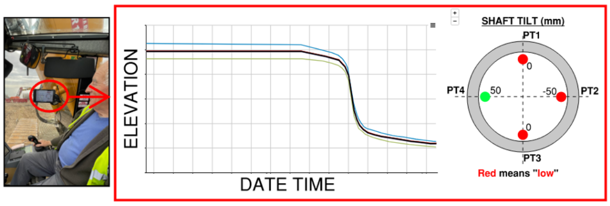

Fig. 8: Ward and Burke LLS interface as utilised on-site during construction [6].

The ultimate objective during construction of the caisson was to achieve the target embedment depth while temporarily ensuring the caisson wall reached a sufficient height to accommodate additional wall construction. A braking system was incorporated into each wall pour to account for uncertainty in soil parameters and limit excessive movement during construction in the event of bearing failure.

3 Results and discussion

The findings of the study are presented in the following sections.

3.1 Analytical assessment

The closed-form analytical results estimate the construction stage at which applied loading exceeds the bearing resistance of the soil. They also predict the depth of embedment required before vertical equilibrium is restored and the caisson ceases sinking. The analysis predicted a bearing failure would occur prior to the completion of wall construction for both strength profiles of the ACS layer. Fig. 9 presents the response for DL 1 and DL 2, plotted against each concrete pour. The applied load and bearing resistance are shown on the primary axis, with the embedment associated with bearing failure indicated on the secondary y-axis.

For DL 1, the trigger load is predicted to occur between pours 3 and 4, with failure developing during this load increment. Completion of pour 4 corresponds to a calculated embedment requirement of 3.4 m to restore stability and permit continuation of construction. For DL 2, the same response is obtained, although the higher initial resistance delays the trigger condition until the fifth pour, resulting in a calculated embedment of 4.2 m.

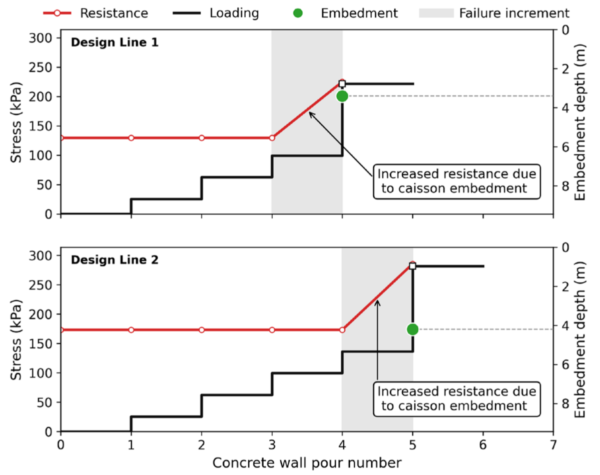

Fig. 9. Analytical bearing capacity assessment results for DL 1 and DL 2.

3.2 FEA model results

Finite element results for the two strength profiles are presented in terms of bearing response and associated deformation patterns at the governing load stage. For DL 1, the computed bearing capacity of 320 kPa is lower than the applied stress of 363.9 kPa, indicating that penetration would initiate during wall pour 7. In contrast, DL 2 provides a higher bearing capacity (370 kPa) which exceeds the applied load, indicating that stability would be maintained throughout wall construction.

The strength reduction method in PLAXIS was used, whereby the soil's undrained shear strength is progressively reduced until failure, identified by numerical non-convergence and rapidly increasing displacements [17]. The deformation contours shown in Fig. 10 represent the final calculation step prior to failure and indicate the mobilisation of a bearing failure mechanism beneath the caisson base. For strength profile DL1, the displacement field forms a broad bulb beneath the caisson wall, with the principal shear zone extending inward towards the shaft centre (Fig. 10 (a)). In the stronger profile (DL2), deformation remains concentrated beneath the base, with a slightly more confined displacement field (Fig. 10 (b)). While the overall failure mechanism is similar in both cases, the weaker profile results in a more extensive deformation zone.

3.3 Observed performance and discussion

The caisson was constructed to full height without any significant penetration into the working platform of clean stone. Displacement was not observed until surcharge excavation commenced. This indicates that the in-situ undrained shear strength profile exceeded that assumed in DL 1 and DL 2. The characteristic strengths adopted at design stage therefore appear conservative relative to field behaviour. The FEA model utilising DL 2 proved most accurate for predicting the trigger load (Table 7).

Closed-form bearing capacity calculations were significantly more conservative than both the FEA predictions and the observed field behaviour. Classical bearing capacity solutions assume instantaneous mobilisation of a fully developed failure mechanism and therefore do not capture the progressive stress redistribution that occurs during loading, including incremental mobilisation of end bearing resistance and lateral confinement from the surrounding soil. The finite element model therefore produced predictions more consistent with the observed trigger load.

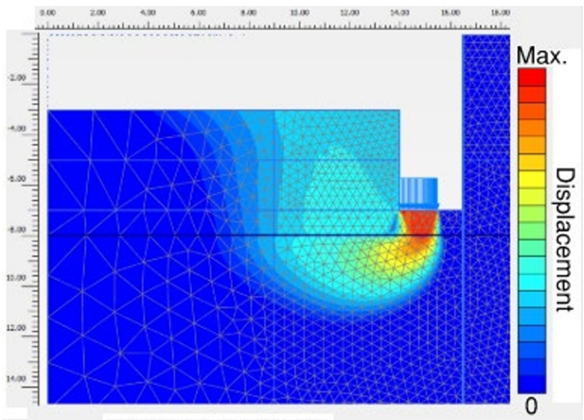

(a) DL 1 bearing failure displacement results.

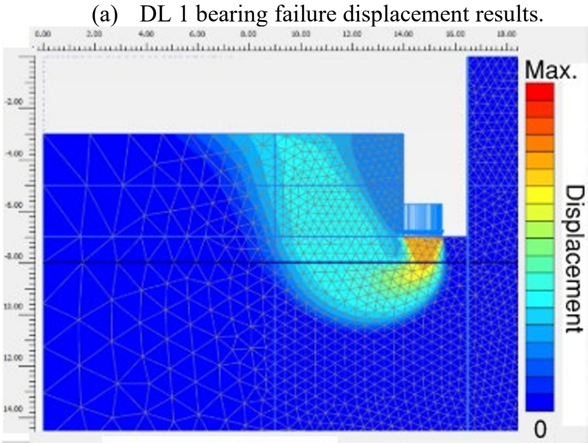

(b) DL 2 bearing failure displacement results.

Fig. 10. FEA incremental displacement results for DL 1 (a) and DL 2 (b), illustrating the failure plane for each design line strength in the axisymmetric model.

Table 7. Summary of results.

	Trigger Load Bearing Capacity (kPa)		
Design line	Analytical	FEA	Observed
1	129.4	320	>364
2	173.1	370	

Post-construction processing of the LLS monitoring data enabled reconstruction of the shaft sinking sequence. Fig. 11 (a) presents shaft elevation with time, while Fig. 11 (b) illustrates the variation in tilt with elevation. Initial embedment occurred following removal of approximately half of the clean stone surcharge (≈ 1.7 m). Once the trigger load was reached and failure commenced, the caisson sank into the clay by 2.9 m in approximately five minutes. Back-analysis using the analytical framework outlined in Section 4.1 indicates an initial undrained shear strength of approximately 28 kPa at 30 mOD, corresponding to 3.0 and 1.75 times those adopted for DL 1 and DL 2, respectively.

The monitoring system provided over 2.5 hrs advance notification of impending movement of the caisson as the surcharge material was excavated from inside the shaft. Progressive creep was recorded (Fig. 11 (c)), with displacement notably accelerating from 12.1 mm hr^{-1} to 64 mm hr^{-1} in the final 30 minutes prior to the full shear strength of the soil being mobilised. This response is consistent with the ductile behaviour typically exhibited by soft cohesive soils and supports the application of an observational approach for open caisson construction in such ground conditions.

As anticipated, once the trigger load was reached the structure penetrated through the clean stone surcharge, with the precast wedges progressively failing inward as contact with the underlying clay was mobilised. Site observations revealed base heave as the slip surface extending towards the caisson centre.

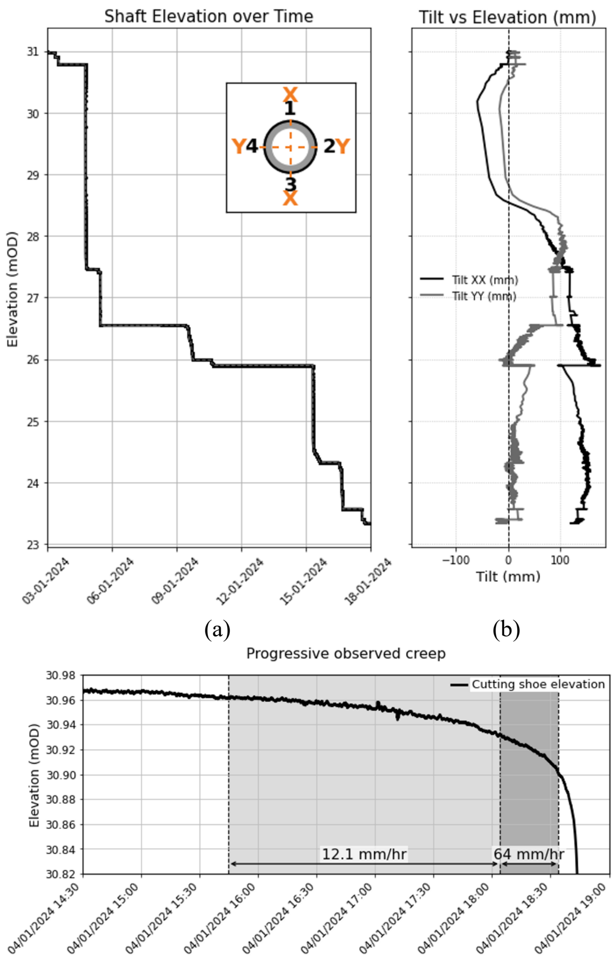

(c)

Fig. 11. (a) and (b) Observed results of caisson movements for initial sinking; and (c) Observed creep before soil failure indicating ductile behaviour of soft clays.

The initial movements within the soft clay highlight the practical challenges associated with maintaining verticality during penetration (Fig. 11 (b)). The reinforced concrete guide collar proved effective in limiting lateral deviation during early sinking stages. In practice, verticality was achieved by correcting tilt utilising the instrumented level system.

4 Conclusions

This study investigated the bearing response of soft clay beneath a caisson during the construction stage prior to shaft sinking. The aim was to predict trigger loads that would lead to premature bearing failure during construction. Closed-form analytical methods and FEA were used to estimate trigger thresholds to support an observational framework informed by real-time field monitoring data.

The principal conclusions of the study are:

1. Analytical and numerical model predictions of the trigger load at which the caisson would start sinking were conservative. The closed-form calculations underestimated field performance by factors >2.8 and >2.1 for DL 1 and DL 2 respectively. The FEA model incorporating DL 1 underestimated the bearing capacity of the soil by a factor >1.13, while DL 2 most closely represented the trigger loads observed in the field.
2. Back-analysis of the monitored sinking response indicates the in-situ undrained shear strength of the soil was significantly higher than that assumed at design stage.
3. The increased soil strength may be attributed to the induced over-consolidation associated with the excavation of the landfill deposits and site dewatering. Secondary influences such as strain-rate effects, anisotropy and spatial variability of soil properties may also have contributed.
4. Penetration occurred by punching through the clean stone working platform prior to mobilisation of clay resistance, followed by inward wedge failure and development of a slip surface beneath the caisson, consistent with the mechanisms inferred from analytical and numerical modelling.
5. Field instrumentation demonstrated the ductile behaviour of very soft clays by indicating creep over a sustained period prior to bearing failure during surcharge unloading.
6. The findings demonstrate the value of integrating analytical methods, numerical modelling and observational monitoring for caisson construction in soft clay, where consolidation and construction processes can significantly modify in-situ soil behaviour and the governing failure mechanisms.

The authors gratefully acknowledge the technical guidance and financial support provided for this research by Ward & Burke Construction Ltd., as well as the efforts of the site team at the Athlone Main Drainage Scheme.

References

1. Uisce Éireann, Supporting Housing. https://www.water.ie/projects/strategic-plans/supporting-housing.
2. D. Allenby, G. Waley, and D. Kilburn, Examples of open caisson sinking in Scotland. Proc. Inst. Civ. Eng. - Geotech. Eng. **162**, 59-70 (2009). https://doi.org/10.1680/geng.2009.162.1.59
3. R. Royston, B. B. Sheil, and B. W. Byrne, Monitoring the construction of a large-diameter caisson in sand. Proc. Inst. Civ. Eng. - Geotech. Eng. **175**, 323-339 (2020). https://doi.org/10.1680/jgeen.19.00266
4. Judgment of the Court (Tenth Chamber). https://infocuria.curia.europa.eu/tabs/document?source=document&text=&docid=212353&doclang=EN.
5. Uisce Éireann, Athlone Main Drainage Scheme. https://www.water.ie/projects/local-projects/athlone-main-drainage-s.
6. L. Willis, R. Royston, and D. Phillips, Utilising instrumentation to monitor the construction of a large underground shaft in Ireland. Proc. 20th Sensors and Their Applications Conf. (University of Limerick, 2024). https://doi.org/10.34961/RESEARCHREPOSITORY-UL.29290949.V1
7. M. M. Long and N. J. O'Riordan, Field behaviour of very soft clays at the Athlone embankments, Géotechnique **51**, 293-309 (2001). https://doi.org/10.1680/geot.51.4.293.39401
8. T. Lunne, P. K. Robertson, and J. J. M. Powell, Cone Penetration Testing in Geotechnical Practice (Blackie Academic & Professional, London, 1997).
9. B. Look, Handbook of Geotechnical Investigation and Design Tables (Taylor & Francis/Balkema, Leiden, The Netherlands, 2007).
10. R. Whitlow, Layered Deposits, in Basic Soil Mechanics, 3rd edn. (Addison Wesley Longman Limited, 1995), pp. 465–466.
11. EN 1997-1:2004+A1:2013 Eurocode 7 — Geotechnical design — Part 1: General rules, (2013).
12. R. Royston, B. B. Sheil, and B. W. Byrne, Undrained bearing capacity of the cutting face for an open caisson. Géotechnique, **72**, 632-641 (2022). https://doi.org/10.1680/jgeot.20.P.210
13. R. Royston, Monitoring the Construction of a Large Diameter Caisson in Clay, in Proc. 26th Eur. Young Geotech. Eng. Conf. (Austria, 2018), pp. 161–170.
14. PLAXIS, PLAXIS 2D Material Models Manual, (Bentley Systems, n.d.).
15. F. M. Abdrabbo and K. E. Gaaver, Applications of the observational method in deep foundations. Alex. Eng. J. **51**, 269-279 (2012). https://doi.org/10.1016/j.aej.2012.10.004
16. B. Sheil, R. Royston, and B. Byrne, Real-time monitoring to inform the construction of large-diameter caissons, in Proc. China-Europe Conf. Geotech. Eng. (Vienna, Austria, 2018).
17. PLAXIS, PLAXIS 2D Reference Manual, Bentley Systems, 2022, Section 7.3.5 – Safety calculation (phi/c reduction)